DOI: 10.21062/mft.2025.038 http://www.journalmt.com

Effect of Thermal Ageing on Changes in Modulus of Elasticity E Measured by Ultrasound, Bending Test and EBSD

Jana Vesela (0000-0002-2314-634X), Petr Beneš (0000-0001-5673-0588), David Bricín (0000-0002-9354-2751)
Research Centre Rez, Morseova 4, 301 00 Plzen, Czech Republic. E-mail: jana.vesela@cvrez.cz

The materials used in VVER nuclear power plants are subject to thermal ageing in operation, among other degradation mechanisms. The aim of the experiment was to verify the effect of thermal ageing on the change of ultrasound velocity on the extracted parts of main circulation piping and pressurizer surge line made of austenitic steels. Two steel conditions were evaluated, as received and thermally aged. The research was carried out on samples made from non-operated pipelines and samples from pipelines after 28 years of operation. The samples were subjected to thermal ageing at 450 °C in an atmospheric furnace with a specified exposure time to simulate extended operation of the component for 60 years, where 1 year of operation means 10 months at 100 %-unit power and 2 months in shutdown. The samples were subjected to ultrasonic property measurements and the longitudinal and transverse wave velocities obtained are further used to calculate the Poisson's constant and elastic modulus E of the material. To verify the ultrasonic measurements, the samples were also subjected to mechanical tests to verify the changes in the mechanical properties in terms of elastic behaviour of the selected steels when subjected to a static 3-point flexural test and Electron backscatter diffraction analysis (EBSD).

Keywords: Ultrasound speed, Thermal ageing, Elastic modulus E, Tree-point flexural test, Elastic stiffness coefficient

1 Introduction

Methods and selected non-destructive testing (NDT) techniques can be used to detect defects and possibly characterize material properties. They offer several advantages over destructive techniques based on sampling and testing. Ultrasonic testing (UT) is one of the widely used methods for operational inspections at power plants for the detection and characterization of cracks. The article deals with the use of Pulse-echo UT technique also for the purpose of detecting structural changes in a material that lead to a change in Young's modulus of elasticity E. Measurements of ultrasound properties such as applied wave propagation velocity and attenuation can be used to determine changes in the microstructure and subsequently the modulus of elasticity of the tested material.

Advantageously, this type of measurement can be used to verify material processing procedures during production and to detect possible degradation of the material during operation. In order to determine the structural change in the state of the material, it is essential to measure the properties in the initial state for comparison with the in-service results. Results of calculated the modulus of elasticity based on measured UT parameters has been verified by mechanical tests and EBSD.

2 Test samples

Two materials 08Ch18N10T (sample 1) and 08Ch18N12T (sample 2) were selected for testing. These are the materials used to make pressurizer surge line and main circulation piping the VVER type nuclear power plant. The samples for the testing are described in Table 1. The initial (as received) state is indicated by the letter I and the thermally aged state by A. The dimensions of the sample, the number of measuring points for UT and the thermal exposure time at 450 °C are also given. Each sample was then cut into two identical halves in the direction of the pipe axial axis.

Tab. 1 *Samples description*

Sample No.	Material	Marking	Type and status	Dimensions [mm]	Aging time at 450 °C	No. of measuring points
1-I	08Ch18N10T	1-Ia	initial	125x67x20	-	18
		1-Ib	initial - annealed		1085 h	
1-A	08Ch18N10T	1-Aa	28 years in operation	105x90x18	-	20
		1-Ab	28 years - annealed		1240 h	
2-I	08Ch18N12T	2-Ia	initial	180x125x35	-	40
		2-Ib	initial - annealed		2165 h	
2-A	08Ch18N12T	2-Aa	28 years in operation	285x185x35	-	44
		2-Ab	28 years - annealed		2474 h	

One half of the sample was used to measure the initial (unaffected) or post-delivery condition (i.e., after 28 years of service) in Table 1, labeled (a), and the other half of samples 1 and 2 were used for subsequent thermal aging with label (b).

3 Methodology of ultrasonic testing

The Pulse-Echo ultrasonic testing (P/E) methodology is based on the measurement of the propagation velocity of longitudinal and transverse waves (c_L and c_T) of the material before and after thermal ageing. The obtained values are used to calculate the Poisson's number and the modulus of elasticity (E) according to the following equations (1) and (2):

Poisson's number:

$$v = \frac{1 - 2(\frac{c_T}{c_L})^2}{2 - 2(\frac{c_T}{c_L})^2} \quad (1)$$

Where:

c_T …Velocity of transversal waves [m/s],

c_L …Velocity of longitudinal waves [m/s].

The modulus of elasticity E [GPa]:

$$E = \frac{{c_L}^2 \rho(1+v)(1-2v)}{1-v} \quad (2)$$

Where:

ρ …Density of material [kg/m³].

The measurements were carried out by the Pulse-Echo ultrasonic technique using direct probes of longitudinal and transverse waves with a frequency of 5 MHz and a transducer diameter of 12.7 mm. The velocity of ultrasonic propagation is one of the main properties of the material in terms of non-destructive testing, and its change indicates a possible change in the structure of the tested material. Ultrasonic velocity measurements were made at each measuring point and the thickness of the material at the measured point determined by 3D scanning of the samples was used for the precise thickness calibration. At the same time, the second back-wall echo drop was recorded at the measuring point and the values obtained were used to calculate the ultrasonic beam attenuation.

4 Ultrasound measurement results

The results of the longitudinal and transverse wave velocity measurements at each measuring point before and after thermal exposure were recorded and graphically displayed, including their progression using a trend line. The measured values of c_L and c_T before and after exposure are graphically compared with each other, as well as the attenuation values.

A fixture with a 500 g weight was used to fix the probe to ensure constant pressure of the probe to the outer tested surface. For the graphical representation of the ultrasound velocity waveform and its moving average was selected sample 2-Ia and 2-Ib, see Fig. 1 and 2. For comparison, the results of sample 2-Aa and 2-Ab are shown in Figs. 3 and 4.

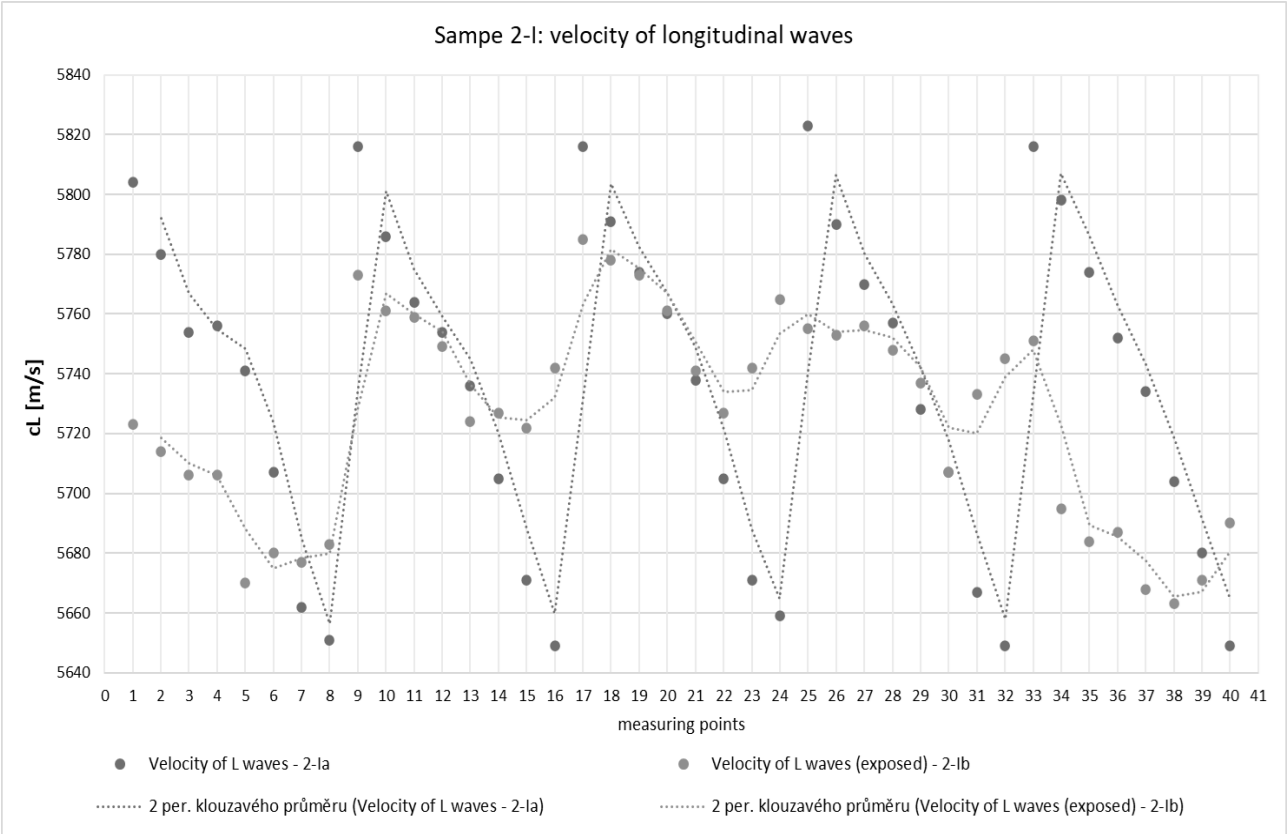

Fig. 1 *Sample 2-I – velocity of L waves (2-Ia in blue and 2-Ib in orange)*

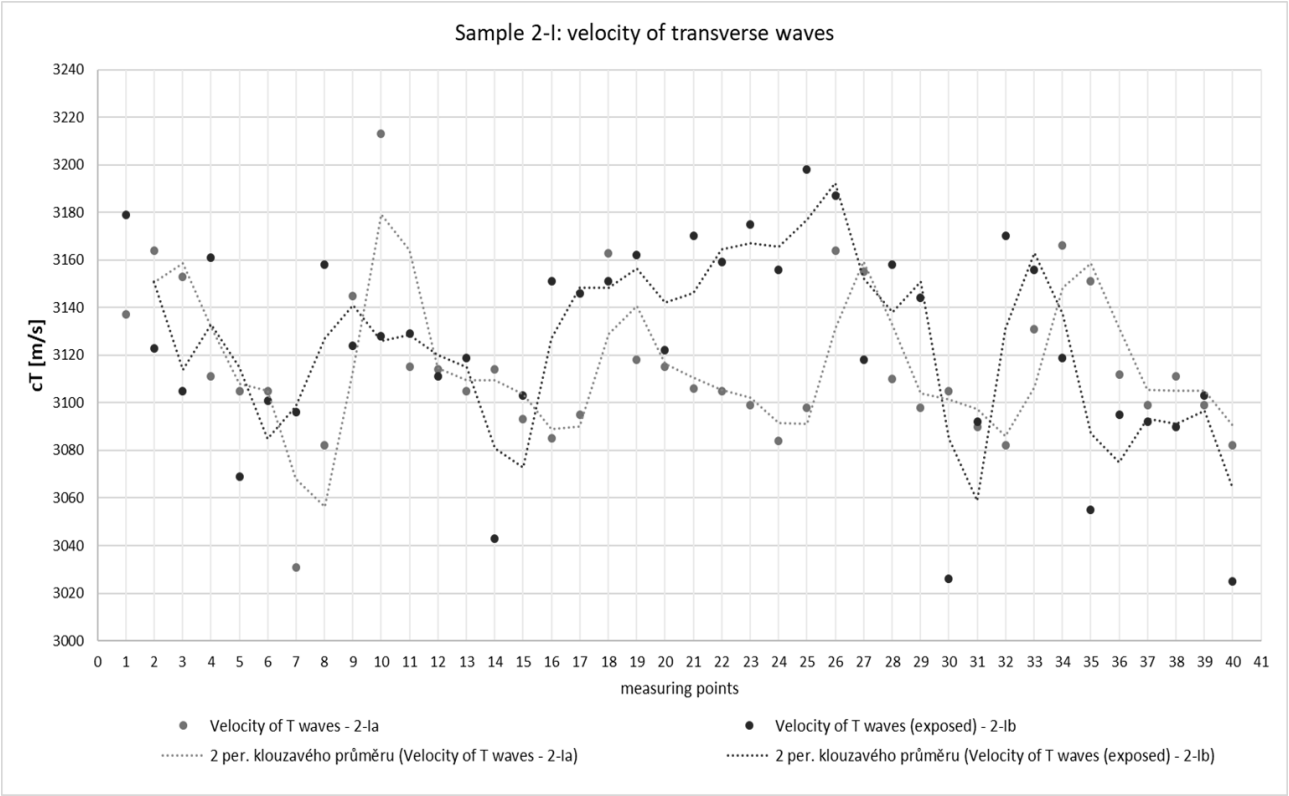

Fig. 2 *Sample 2-I – velocity of T waves (2-Ia in green and 2-Ib in red)*

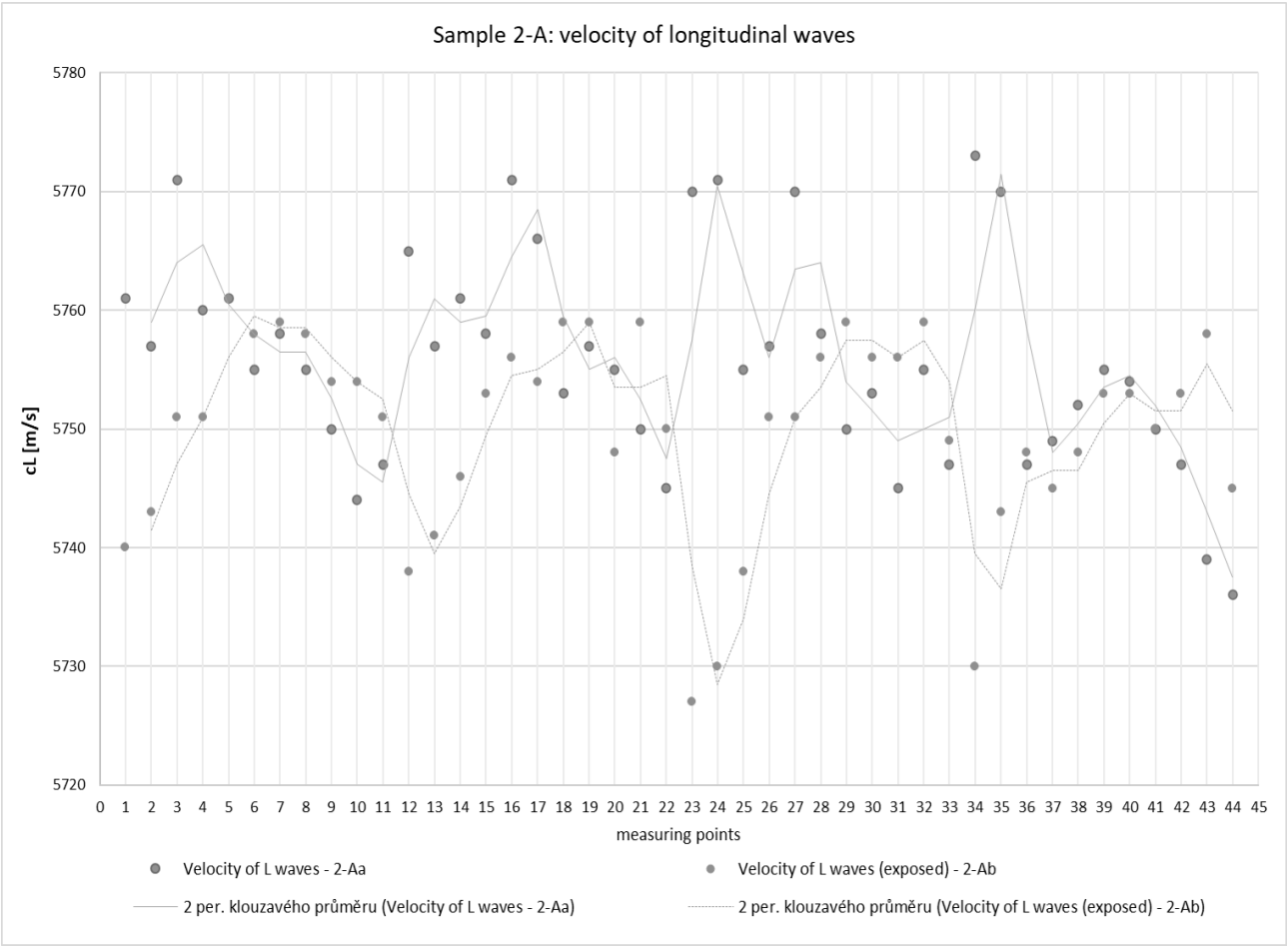

Fig. 3 *Sample 2-A – velocity of L waves (2-Aa in blue and 2-Ab in orange)*

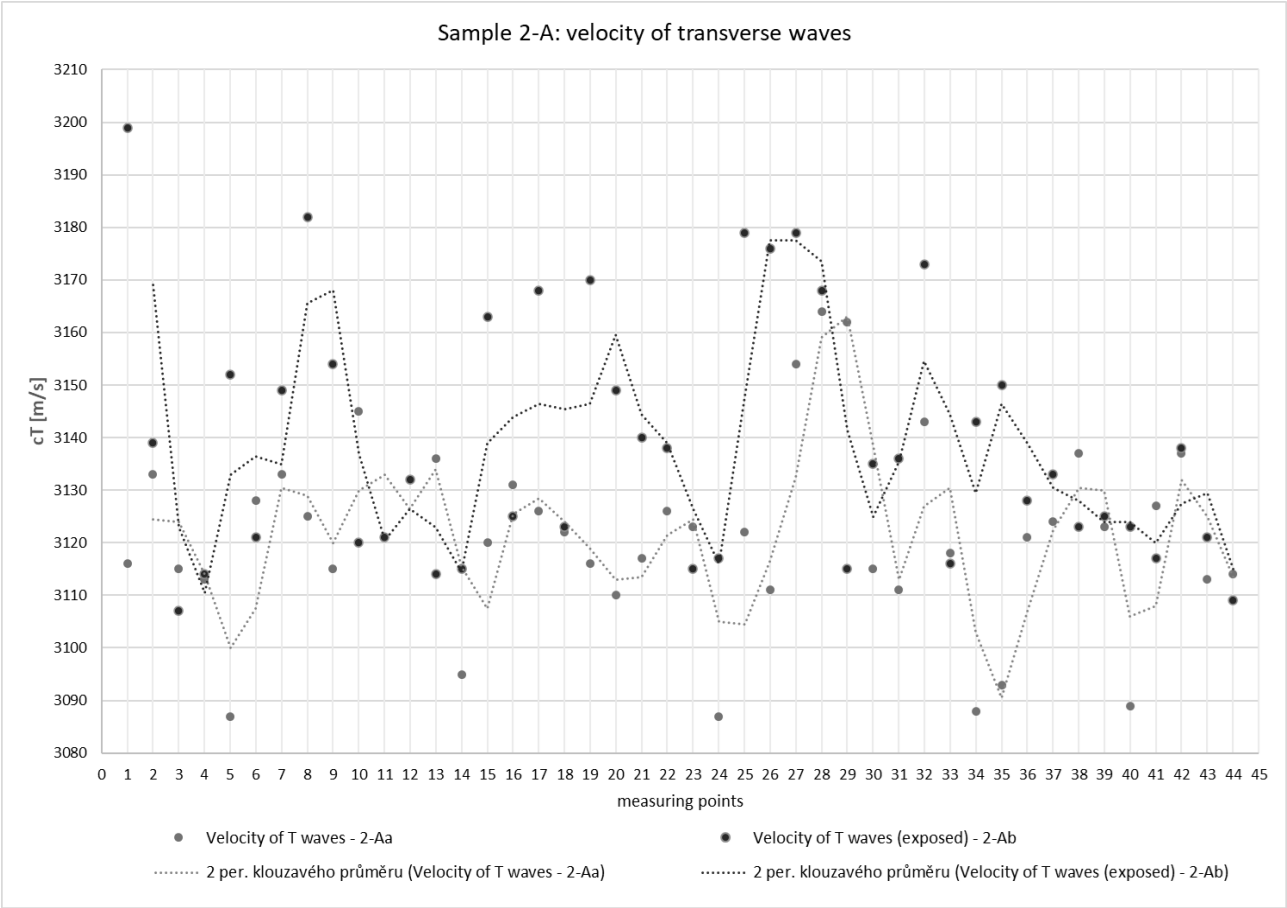

Fig. 4 *Sample 2-A – velocity of T waves (2-Aa in green and 2-Ab in red)*

The results of both samples and all states, Ia - initial state, Ib - delivered state from operation, Aa – post-delivery condition, Ab – post-delivery condition exposed, are summarized in Table 2 for values of ultrasound velocities, Poisson number and modulus of elasticity E. Equation (1) was used to calculate the Poisson's number and equation (2) was used to calculate the modulus of elasticity E.

Tab. 2 *Modulus of elasticity E measured by UT*

Sample No.	c_L (m/s)	c_T (m/s)	υ	E (GPa)
1-Ia	5759 ± 30	3144 ± 33	0.287 ± 0.003	143.3 ± 3.3
1-Ib	5763 ± 35	3147 ± 28	0.287 ± 0.002	143.5 ± 2.7
1-Aa	5746 ± 26	3145 ± 16	0.286 ± 0.001	143.5 ± 1.5
1-Ab	5662 ± 93	3079 ± 60	0.290 ± 0.002	137.2 ± 5.5
2-Ia	5736 ± 60	3115 ± 61	0.291 ± 0.005	141.2 ± 6.0
2-Ib	5726 ± 41	3124 ± 58	0.288 ± 0.007	142.3 ± 5.8
2-Aa	5756 ± 12	3121 ± 26	0.292 ± 0.004	141.7 ± 2.7
2-Ab	5750 ± 11	3139 ± 31	0.287 ± 0.005	143.7 ± 3.3

5 Bending test and determination of the flexural modulus

To verify the values of the elastic modulus determined by the ultrasonic method, the determination of the elastic modulus was carried out using mechanical tests - static bending tests. In order to determine the flexural modulus, a static three-point flexural test was performed. The specimens used were rectangular cross-section (4 mm width and 3 mm height). The distance between the supports was 40 mm. The loading rate was chosen to be 10 MPa/s. The radius of the bending rollers was 10 mm. The radius of the indented mandrel was 10 mm. The contact point between the mandrel and the specimen surface was not lubricated. Similarly, the contact point between the surface of the sample and the surface of the roller was not lubricated. The measurements were carried out on a Zwick/Roell Z005 universal tensile machine.

When comparing the values of the bending modulus from the three-point bending test and the modulus of elasticity E determined by ultrasonic testing, it must be remembered that the moduli determined in this way are fundamentally different. This difference results from the different nature of the individual testing methods. The bending of the body represents the combined tensile and compressive stresses on the body, which corresponds to the transmission mechanism of the longitudinal ultrasonic wave in the material, whereby tensile and compressive regions are formed in the material. In contrast, in the case of transverse ultrasonic waves, this mode of transmission of mechanical vibrations in the material is not applied (in this case, there is a shear mechanism of ultrasonic wave penetration).

Two modes of testing method were implemented. In the first case, the specimens were loaded in the elastic deformation region in the stress range 0 - 200 MPa. In this stress range, the values of the bending modulus were determined from the characteristic stress-strain curve using different methods: secant modulus, tangent modulus and chord modulus. Furthermore, the flexural modulus determined from the hysteresis curve was determined by this testing method. This hysteresis loop was created by unloading the specimen at an upper load limit of 180 MPa and then loading it at a lower stress limit of 30 MPa. In this way, a hysteretic loop was created where the slope of tje line formed by connecting the lower and upper intersection of the loop gives the value of the hysteresis flexural modulus $E_{hysteresis}$.

The second method of measuring the flexural modulus consisted in consuming a certain proportion of the plastic deformation of the specimen. For this reason, prior to the actual measurement of the specimens, these specimens were subjected to a three-point cyclic flexural load in the stress range 0 - 70 MPa. The number of loading cycles was 30 for each specimen measured. The main reason for performing this cyclic preloading of the specimens was to make the determination of the flexural modulus more precise by exhausting a certain level of plasticity of the examined material. Subsequently thus cycled samples were subjected to the same loading regime to determine the flexural modulus as in the first testing method.

Table 3 summarizes the measured flexural modulus values for the individual materials. The values are calculated as mean values from modulus determined by the tangent, secant, chord/regression and hysteresis loop methods. As can be seen from the measured data in Table 3, the depletion of the plasticity of the specimens induced by cyclic loading always leads to a decrease in the value of the flexural modulus. Furthermore, it was not found that the thermal aging of the tested samples led to an influence on their flexural modulus. The measurements also revealed that the flexural modulus of material 08Ch18N10T is practically identical to that of 08Ch18N12T in both methods of measuring the flexural modulus.

Tab. 3 *Flexural modulus*

Sample no.	Flexural modulus [GPa] / first method	Flexural modulus [GPa] / second method (cycled samples)
1-Ia	159.8 ± 1.6	145.9 ± 2.8
1-Ib	160.7 ± 1.5	133.4 ± 3.8
1-Aa	155.7 ± 2.8	143.9 ± 4.4
1-Ab	154.2 ± 2.7	141.3 ± 5.3
2-Ia	153.7 ± 1.1	140.8 ± 3.0
2-Ib	156.6 ± 1.8	143.4 ± 4.0
2-Aa	153.0 ± 3.4	141.3 ± 4.0
2-Ab	154.7 ± 1.7	141.8 ± 4.9

6 EBSD and Young's modulus

Surface of specimens was prepared by grinding and polishing using Tegramin 30 grinding machine in combination with SiC grinding foils with grit in range of 220-2000 and MD-Nap polishing plates in combina-tion with diamond suspensions with particle sizes in range of 1-9 μm. OP-S suspension with particle size of 0.25 μm was used for final polishing step before analysis. Specimens for analysis was pretilted by 70° during measurement.

Measurement was done by Tescan Mira 3 scanning electron microscope using secondary electron (SE) mode, accelerating voltage 15 kV, working distance 20 mm. and view field of 500 μm. Electron backscatter diffraction analysis (EBSD) was done using Nordlys-Nano detector with camera set to 8x8 mode with step size of 0.98 μm. Oxford Aztec software was used to collecting EBSD patterns. Obtained data was processed using AztecCrystal software 3.1.

It is possible to use a Reuss, Voigt, Hill, or Geometric model to calculate Young's modulus in Aztec Crystal software based on elastic stiffness coefficients (ESC) C11, C12, and C44. Three variants of elastic stiffness coefficinent were choosen from literature, see Table 4. The first one was choosen as reference

for austenitic steel regardless to chemical composition of analysed samples. Other vari-ants were chosen according to it.

Another elastic stiffness coefficients were calculated based on wave velocity mesurements during ultrasonic testing (UT) and using equestions 3-5 [11-14].

Tab. 4 *Elastic stiffness coefficients used for Young modulus calculation*

ESC variant no.	C11	C12	C44	Ref. no.
(1)	192.3	128	116.4	[11]
(2)	207	132	123	[12]
(3)	215.9	144.6	128.9	[15]

$$C_{11} = \rho \cdot v_l^2 \quad (3)$$

$$C_{44} = \rho \cdot v_t^2 \quad (4)$$

$$A = \frac{2 \cdot C_{44}}{C_{11} - C_{12}} \quad (5)$$

Where:
ϱ…Mass density (kg/m^3);
v_l, v_t…Sounds velocity (m/s);
A…Zener elastic anisotropy (dimensionless).
Table 5 then summarised calculated stiffness coefficients C_{11}, C_{12}, and C_{44}.

Tab. 5 *Calculated elastic stiffness coefficients (ESC variant no. 4)*

Sample no.	C11	C12	C44
1-Ia	2.620	2.178	0.781
1-Ib	2.624	2.180	0.782
1-Aa	2.608	2.166	0.781
1-Ab	2.533	2.108	0.749
2-Ia	2.616	2.179	0.771
2-Ib	2.607	2.167	0.776
2-Aa	2.634	2.195	0.774
2-Ab	2.628	2.168	0.814

Table 6 summarizes the average values of the calculated Young modulus by the Reuss method and Hill for ESC variant no. 4, which better fits with other measurements of Young modulus. Young modulus may chan-ge based on the elastic stiffness coefficient used and due to the calculation model used for its calculation. In this case, based on the calculation model, the Young modulus values differed by up to 56.8±4.1 GPa and due to use of different variant of ESC by up to 68.8±5.3 GPa. Regardless of the value of ESC, the results indicate minimal diference in the value of Young's modulus for all groups of samples regardless of years in operation or annealing procedure.

Tab. 6 *Average values of calculated Young modulus based on different elastic stiffness coefficients*

Method	Reuss [GPa]				Hill [GPa]
Sample no./ ESC variant no.	(1)	(2)	(3)	(4)	(4)
1-Ia	150 ± 0.5	169.2 ± 0.5	167.3 ± 0.5	109.4 ± 0.4	134. 6± 0.5
1-Ib	149.7 ± 1.1	168.1 ± 1.1	166.2 ± 1.2	108.7 ± 0.8	133.9 ± 1
1-Aa	152.2 ± 2.8	170.7 ± 2.9	169 ± 3.1	110.9 ± 2.1	136.2 ± 2.5
1-Ab	151.9 ± 0.2	170.5 ± 0.2	168.7 ± 0.2	106.4 ± 0.1	130.6 ± 0.2
2-Ia	159.2 ± 2.2	177.9 ± 24.1	176.7 ± 2.4	115 ± 1.6	141.2 ± 1.9
2-Ib	139 ± 5.1	157 ± 5.4	163.4 ± 0.5	100.4 ± 3.9	122.1 ± 4.8
2-Aa	160.8 ± 14.7	179.5 ± 15.2	178.6 ± 16.4	116.8 ± 11.2	136.3 ± 12.8
2-Ab	167.2 ± 6.2	186.1 ± 6.3	185.6 ± 6.8	127.2 ± 4.9	153.1 ± 5.4

The difference between the Young's modulus values obtained by EBSD and the other techniques used depends mainly on the mathematical model that was used to predict the polycrystalline elastic constant by averaging the single crystal elastic coefficients. Another factor that played a role was the relatively small area analyzed in EBS compared to the volumes tested in UT and three-point bending. Thus, differences in the tested volume of the thermally affected material may have affected the EBSD results.

7 Summary

The results of the elastic moduli obtained for the materials tested by the Pulse-Echo ultrasonic technique and three-point flexural test using cycled specimens are compared with each other in Table 7.

When using EBSD measurements, the effect of the small volume of the material under test on the results needs to be taken into account. The selected SW approaches to calculate the Young's modulus using the Reuss and Hill methods for chosen ESC variant give comparable results to the ultrasonic and three-point bending methods, see Table 7.

The values of modulus E obtained from the non-destructive Pulse-Echo ultrasonic technique are consistent with the values of E measured in the mechanical, i.e. destructive, tests of both materials. When comparing the values of the modulus of elasticity E measured by the Pulse-echo technique and the flexural test, it must be ensured that the specimens taken for the mechanical tests are oriented in the same direction as the direction of sounding during the UT method.

The main conclusion of all the above results and conclusions is that formulas (1) and (2) using the measured values of c_L and c_T have been confirmed as suitable for non-destructive measurement of the elastic moduli of selected types of materials. When measuring longitudinal and transverse ultrasonic velocities at the indicated points, it is necessary to ensure that the measurements are carried out under the same conditions, i.e. the same type of coupling medium and probe pressure. The increase in accuracy of thickness measurement by 3D scanning, which was used to increase the accuracy of calibration of both types of velocities, has also contributed to comparable values with mechanical tests.

Tab. 7 *Comparison modulus of elasticity measured by UT, 3-point bending test and EBSD*

Sample no.	Modulus of elasticity [GPa] / ultrasound (UT)	Flexural modulus [GPa] / second method (cycled samples)	Young modulus [GPa] by Reus (ESC variant no. 1)	Young modulus [GPa] by Hill (ESC variant no. 4)
1-Ia	143.3 ± 3.3	145.9 ± 2.8	150.0 ± 0.5	134.6 ± 0.5
1-Ib	143.5 ± 2.7	133.4 ± 3.8	149.7 ± 1.1	133.9 ± 1.0
1-Aa	143.5 ± 1.5	143.9 ± 4.4	152.2 ± 2.8	136.2 ± 2.5
1-Ab	137.2 ± 5.5	141.3 ± 5.3	151.9 ± 0.2	130.6 ± 0.2
2-Ia	141.2 ± 6.0	140.8 ± 3.0	159.2 ± 2.2	141.2 ± 1.9
2-Ib	142.3 ± 5.8	143.4 ± 4.0	139.0 ± 5.1	122.1 ± 4.8
2-Aa	141.7 ± 2.7	141.3 ± 4.0	160.8 ± 14.7	136.3 ± 12.8
2-Ab	143.7 ± 3.3	141.8 ± 4.9	167.2 ± 6.2	153.1 ± 5.4

Acknowledgement

The presented work has been realized within Institutional Support by Ministry of Industry and Trade of the Czech Republic.

References

[1] KRAUTKRÄMER, J., KRAUTKRÄMER, H., (1990). *Ultrasonic testing of materials*, pp. 13-14, 533-534, Berlin

[2] MOORE, P., (2007). Nondestructive testing handbook, *American Society for Nondestructive Testing*, Vol. 7, pp. 319-321, US

[3] DRUCE, S.G., GAGE, G., JORDAN, G., (1986). Effect of ageing on properties of pressure vessel steels. *Acta metall*, Vol. 34, No.4, pp. 641 – 652. Great Britain. ISBN

[4] EPRI, (2018). Review of nondestructive evaluation methods for damage susceptibility assessment in aging primary loop components. *Technical report 3002013171*, US

[5] WU, S-J., CHIN, P-CH., LIU, H., (2019). Measurement of Elastic Properties of Brittle Materials by Ultrasonic and Indentation Methods. *Applied Sciences*, vol 321, Issue 5887, pp. 385-388.

[6] FRANCO E.E., MEZA J.M., BUIOCHI, F., (2011). Measurement of elastic properties of materials by the ultrasonic through tranismission technique. *DYNA*, vol. 78, No. 168, pp. 58 – 64. Colombia. ISSN 0012-7353

[7] TAI, J.L., SULTAN, M.T.H., LUKASZEWICZ, A., SHAHAR, F.S., TARASIUK, W., NAPIORKOWSKI, J., (2023). Ultrasonic velocity and attenuation of low-carbon steel at high temperatures. *Materials 2023*, 16, 5123.

[8] NANEKAR, P.P., SHAH, B.K., (2003). Characterization of material properties by ultrasonic. *BARC Newsletter*, vol. Issue No. 249.

[9] OLYMPUS / Evident, In: *Elastic Modulus Measurement*. 2002.

[10] BEER, F. P., JOHNSTON, E. R., DEWOLF, J., MAZUREK, D., (2009). *Mechanics of Materials*, McGraw Hill, ISBN 978-0-07-015389-9.

[11] MASUMURA, T., TAKAKI, S. and TSUCHIYAMA, T., (2021). Estimation of elastic stiffness in austenitic stainless steels. In: *Journal of the Society of Materials Science*, Japan, 70(1), pp. 31–34., doi:10.2472/jsms.70.31.

[12] KUČEROVÁ, L., BURDOVÁ, K., JENÍČEK, Š., VOLKMANNOVÁ, J., (2022). Microstructure and Mechanical Properties of 3D Printed Tool Steel after Various Precipitation Hardening Treatments. *Manufacturing Technology*. 22(2):185-191. doi: 10.21062/mft.2022.030.

[13] BECHNÝ, V., MATUŠ, M., JOCH, R., DRBÚL, M., CZÁN, A., ŠAJGALÍK, M., NOVÝ, F., (2024). Influence of the Orientation of Parts Produced by Additive Manufacturing on Mechanical Properties. *Manufacturing Technology*. 24(1):2-8. doi: 10.21062/mft.2024.021.

[14] LEDBETTER, H.M., (1984). Monocrystal-polycrystal elastic constants of a stainless steel, *Physica Status Solidi (a)*, 85(1), pp. 89–96. doi:10.1002/pssa.2210850111.

[15] FENG, J. et al. (2021) 'Isotropic octet-truss lattice structure design and Anisotropy Control Strategies for Implant Application', Materials & Design, 203, p. 109595. doi:10.1016/j.matdes.2021.109595.

[16] BODA, R., PANDA, B., KUMAR, S. (2024) 'Bioinspired design of isotropic lattices with tunable and controllable anisotropy', Advanced Engineering Materials [Preprint]. doi:10.1002/adem.202401881.

[17] TEKLU, A. *et al.*, (2004). Single-Crystal Elastic Constants of fe-15ni-15cr alloy, *Metallurgical and Materials Transactions A*, 35(10), pp. 3149–3154. doi:10.1007/s11661-004-0059-y.